한국표면공학회지
Journal of the Korean Institute of Surface Engineering
Vol. 34, No. 5, Oct. 2001
<연구논문>

An optimized condition for corrosion protection of Type 304 Films prepared by unbalanced magnetron sputtering in 3.5% NaCl solution

Ji-Hong Yoo, Seung-Ho Ahn, Jung-Gu Kim, Sang-Yul Lee*

Department of Advanced Materials Enginieering, Sungkyunkwan University, 300 Chunchun-Dong, Jangan-Gu, Suwon, 440-746, South Korea
**Department of Materials Enginieering, Hankuk Aviation University, 412-791 Koyang, South Korea*

Abstract

Type 304 SS coatings were performed at 200□ onto AISI 1045 carbon steel substrate using unbalanced magnetron sputtering (UBMS) with an austenitic AISI 304 stainless steel (SS) target of 100mm diameter. The total deposition pressure in the active Ar gas was 2×10^{-3} Torr. Coatings were done at various target power densities and bias voltages. Chemical compositions of metallic elements of the coatings were measured by energy dispersive X-rays spectroscopy (EDS). The structure and the morphology of Type 304 SS coatings were investigated by means of X-ray diffraction (XRD) and scanning electron microscopy (SEM). Corrosion properties of the coated specimens were examined using electrochemical polarization measurements and electrochemical impedance spectroscopy in a deaerated 3.5% NaCl solution. The porosity rate was obtained from a comparison of the dc polarization resistance of the uncoated and coated substrates. Scratch adhesion testing was used to compare the critical loads for different coatings.

XRD results showed that the sputtered films exhibit a ferritic b.c.c. α-phase. Potentiodynamic polarization curves indicated that all samples had much higher corrosion potential and better corrosion resistance than the bare steel substrate. The corrosion performance increased with increasing power density and the adhesion was enhanced at the bias voltage of -50V. An improvement in the corrosion resistance can be obtained with a better coating adhesion. Finally, an optimized deposition condition for corrosion protection was found as 40W/㎠ and -50V.

1. INTRODUCTION

The purpose of a surface coating is to provide protection against hazardous environments and, thus, to extend the life time of the protected components. Type 304 stainless steel (SS) coating is often used to protect low alloyed steels against corrosion in aqueous environment[1]. Recently, environmental compliance is becoming a serious issue in surface modification engineering. Vacuum-based plasma processes provide a clean and acceptable alternative[2]. Magnetron sputter deposition[3] is one of the most powerful processes which are now currently and successfully used in many applications, particularly in electronic materials and surface engineering for the production

of films and coatings. It was also used to produce coatings for improved wear, corrosion resistance and other surface properties. Unbalanced magnetron sputter deposition is a further development of the conventional magnetron sputtering to overcome the problem of low deposition rate[4]. A key factor in this system is the ability to transport high ion currents to the substrate. This can enhance the formation of fully dense coatings at a relatively low temperature[5].

Vapor deposited coatings most often exhibit pores and pinholes through which a corrosive attack on the (less noble in most cases) substrate material take place[6-9]. It is obvious that coating characteristics such as density, thickness and porosity rate are important for the corrosion resistance of coated systems, so the measurement of porosity is essential in order to estimate the corrosion resistance of the whole coated component[10, 11]. Additional information on the true surface area can be gained by capacitance measurements using electrochemical impedance spectroscopy[12].

In the this present work, in order to improve the corrosion resistance, we have investigated the relationship of the deposition conditions (power density and bias voltage) of UBMS with the coating characteristics and related corrosion performance.

2. Experimental details

2. 1 Film deposition

The substrate material used in the present inve-stigation was AISI 1045 carbon steel. The chemical compositions of the steel are as follow (in wt %) : 0.45 C, 0.25 Si, 0.75 Mn, 0.03 P, 0.03 S and balance Fe. Coatings were done at 200 □ onto AISI 1045 steel substrate using unbalanced mag netron sputtering. Type 304 SS disc with a diameter of 100㎜ was used as the target. The argon pressure in the vacuum chamber during sputter deposition was maintained at 2×10^{-3} Torr, and the base pressure before admitting the argon was 2×10^{-5} Torr. Before starting the deposition, the substrates were sputter-etched in the deposition chamber at 450V under 1×10^{-2} Torr argon pressure for 10 min to remove the remaining oxide films and to enhance the film's adhesion. Coatings were done at various target power densities (11, 25, and 40 W/㎠), while the bias voltage was fixed as -100 V. After confirming the approximate optimization of target power density based on corrosion test results, coatings were then done at various bias voltages (-0, -50 and -100 V). The major coating characteristics are reported in Table 1.

The structures of the deposited layers were investigated by means of X-ray diffraction (XRD) using Cu Kα radiation. The thickness of the coatings was analyzed by α-step.

Table 1. Values of the coating fabrication parameters.

Sample	Power density (W/㎠)	Bias voltage (V)
C1	11	-100
C2	25	-100
C3a	40	0
C3b	40	-50
C3c	40	-100

2. 2 Electrochemical corrosion test

The corrosion behavior was determined by electrochemical potential-current density measurement. The experiments were controlled by an EG&G 273A potentiostat. A conventional three-

electrode cell was used with the counter electrode made of a platinum rod and a saturated calomel electrode (SCE) as a reference electrode. The test solution for electrochemical investigation was a deaerated 3.5% NaCl solution. The thickness of all coatings was 8㎛ and the test specimens were masked with Amercoat 90 epoxy in order to expose a constant surface area of 0.9㎠.

After an initial stabilization for 2h, the potentiodynamic polarization curves were plotted from -250mV against open-circuit potential (OCP) on the cathodic side and up to +400mV against SCE on the anodic side with a scan rate of 1mV/sec. To insure reproducibility, at least three replicates were run for each specimen.

The A.C. impedance measurements for the coated system were performed with an EG&G 273A potentiostat and a frequency response detector Model 1025 controlled by an electrochemical impedance software (Model 398). Sinusoidal potentials of 5 mV (r.m.s.) around the open-circuit potential, with a frequency range of 100 kHz to 10 mHz were applied to the specimens. The impedance data and corrosion potentials were measured at an interval of 24h over an exposure period of about 200 h. The impedance curves were fit to the coating model using the 'Zview' software and the characteristic coating parameters were determined.

2. 3 Adhesion test

A conventional scratch tester (WS-92 equipped with an acoustic emission detector) was used to evaluate the adhesion of the coating to the substrate. The radius of the diamond pin was 0.2mm. All the tests were performed employing a continuous increase in the normal load, from 0 to 100N, at a loading rate of 100N/min.

2. 4 SEM and EDS

After the immersion test was completed, the surface and corrosion features of coated samples were examined using a scanning electron microscopy (SEM) with qualitative elemental analysis by energy dispersive X-ray spectroscopy (EDS). A qualitative judgment could thus be made concerning the corrosion products at pinhole defects.

3. Results and discussion

3. 1 Characterization of film

X-ray diffraction patterns of Type 304 SS coatings using Cu Kα radiation are presented in Fig. 1.

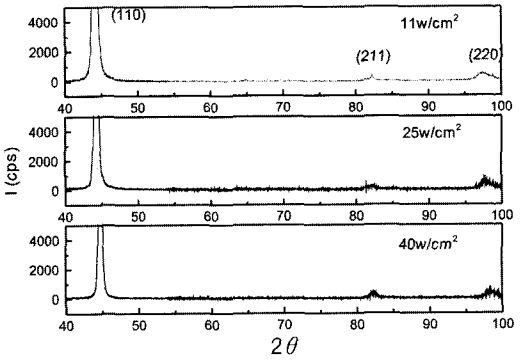

(a)

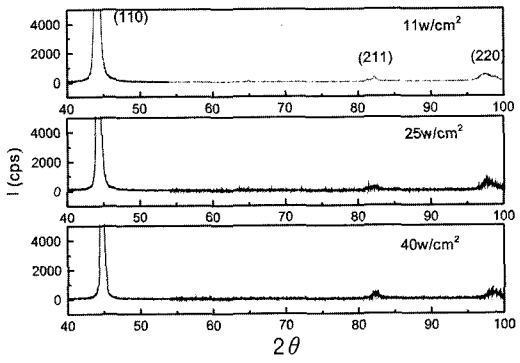

(b)

Fig. 1 XRD analyses of specimens :
(a) at various target power densities,
(b) at various substrate bias voltages.

It clearly showed the three peaks corresponding to a b.c.c. crystallographic structure. Thus, in the case of bulk 304 SS, which is austenitic phase, the sputtered films exhibited a ferritic b.c.c. α-phase. Similar trend was also reported by M. Idiri et al.[13] for films grown by ion beam sputtering. According to Fig. 1, the XRD patterns of coatings were not particularly influenced by deposition conditions. The EDS analysis indicated that the relative Fe, Cr and Ni compositions of all coatings were within the specifications for AISI 304 stainless steel.

3. 2 Study of direct current (d.c) measurement

Potentiodynamic polarization curves for Type 304 SS coatings, measured after 3h of immersion in a deaerated 3.5% NaCl solution, are shown in Fig. 2. The electrochemical characteristics determined from these curves are listed in Table 2. Initially, the potentiodynamic polarization tests were conducted on Type 304 SS films deposited at various power densities, and later on the films deposited at various bias voltages. All samples had much higher corrosion potential and better corrosion resistance than the bare steel substrate. In such a system, where a relatively large noble cathode (Type 304 SS coating) lies over a less noble substrate of small area (AISI 1045 steel), corrosion is expected to initiate rapidly at pores in the coating because of the formation of galvanic cell[14,15]. The increase of a power density caused the decrease in the current density, as shown in Fig. 2(a). This behavior of the coatings could be attributed to an increase in the levels of ion current density that can be achieved at the substrate. This indicated that the high levels of ion bombardment can enhance the formation of fully dense coatings structures[5]. According to Fig. 2(b), the corrosion current density of C3b (40W/㎠, -50V) was lower than others. Therefore, C3b coating had better corrosion resistance than others. Also, C3b alone showed passive behavior with corrosion potential. This particular behavior of C3b was closely related to the adhesion of the interface between the film and the substrate. An improvement in the corrosion resistance can be obtained with a better coating adhesion[8,16]. Table 2 shows the adhesion strength of the coatings obtained

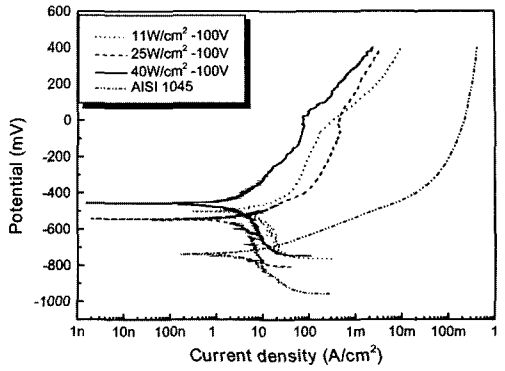

(a)

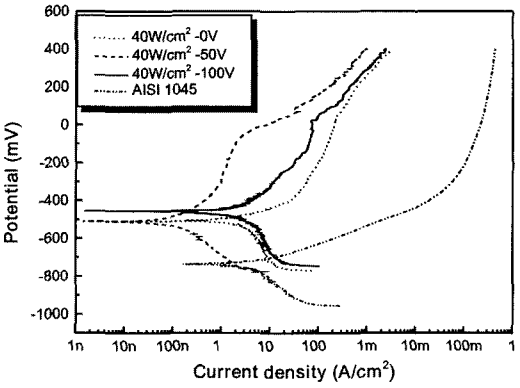

(b)

Fig. 2 Potentiodynamic polarization curves for Type 304 stainless steel coatings: (a) at various target power densities, (b) at various substrate bias voltages.

Table 2. Electrochemical parameters and critical load values of the Type 304 SS coatings on AISI 1045 steel.

Sample	E_{corr} (mV)	i_{corr} (μA/cm^2)	$R_{p,r-u}$ (kΩ cm^2)	Porosity (%)	Critical load (N)
C1	-501.0	13.52	4.55780	0.8672	20
C2	-544.9	4.053	10.1030	0.3912	42
C3a	-508.6	3.793	11.6542	0.3974	10
C3b	-512.7	0.243	266.325	0.0148	78
C3c	-456.9	3.398	18.8181	0.2100	69

from the scratch test. As expected, it seemed to be an enhancement of the adhesion when Type 304 SS coating was deposited at -50V.

3. 3 Study of alternating current (a.c) measurement

The EIS spectra were displayed as Bode plots of the impedance magnitude and of the phase angle as a function of the frequency. Bode plots of Type 304 SS coatings immersed for different periods in a deareated 3.5% NaCl solution, are shown in Fig. 3. These data showed typically two phase constants which were better resolved at larger exposure times. This effect was accompanied by a continuous and slight decrease in the absolute values of the impedance, more noticeable in the low frequ-

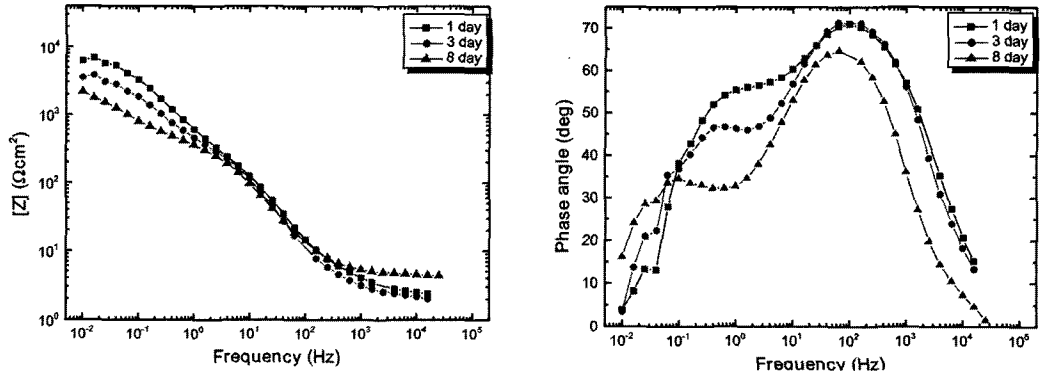

(a) C1 (11 W/cm^2 -100 V)

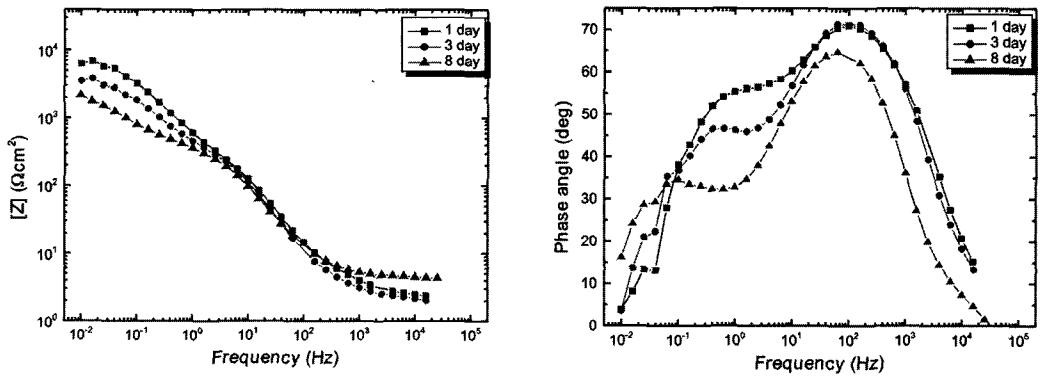

(b) C2 (25 W/cm^2 -100 V)

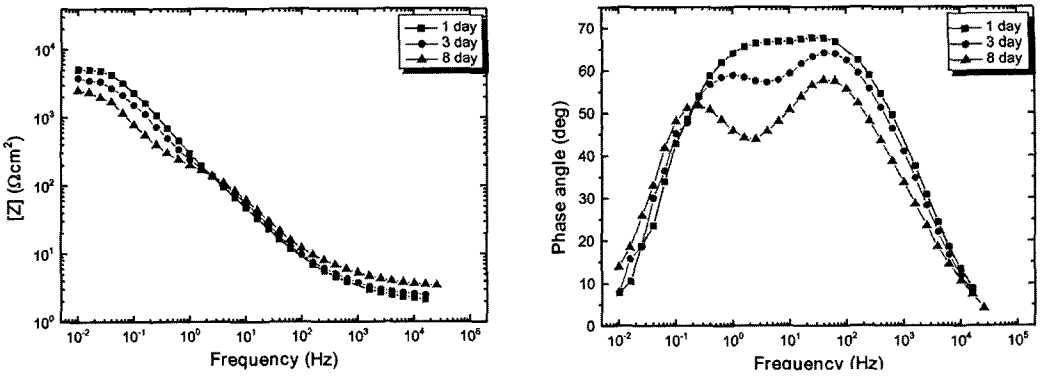

(c) C3a (40 W/cm² -0 V)

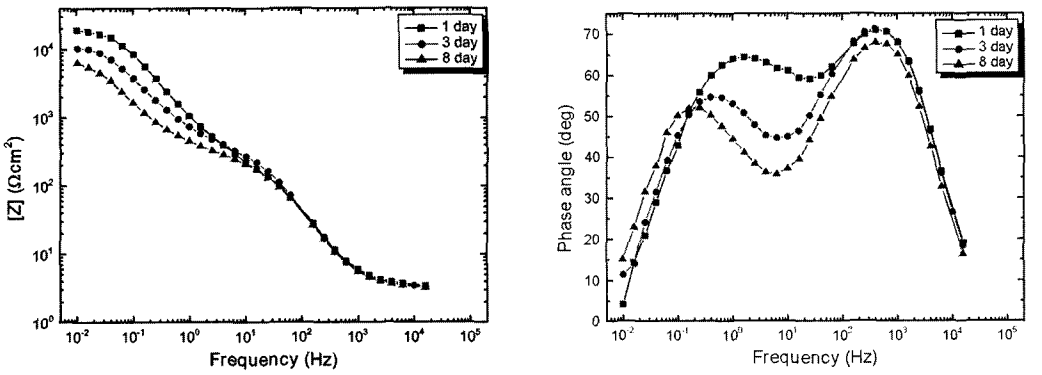

(d) C3b (40 W/cm² -50 V)

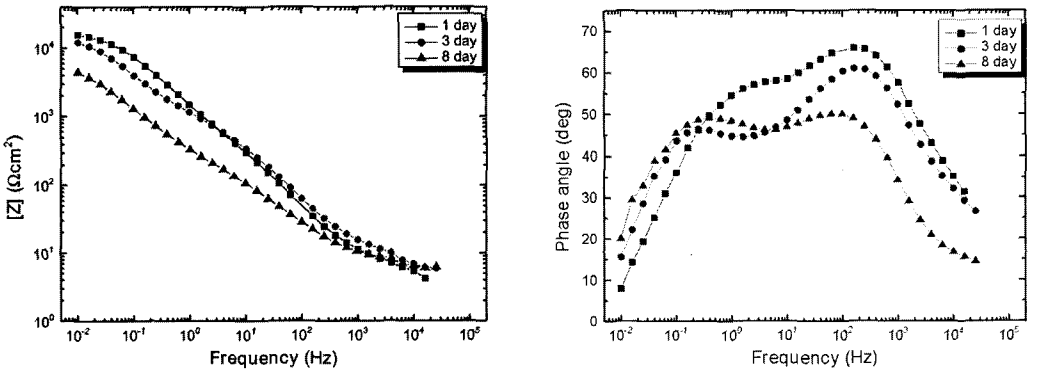

(e) C3c (40 W/cm² -100 V)

Fig. 3. Bode plots for EIS data of Type 304 SS coatings exposed to a deaerated 3.5% NaCl solution at different exposure times.

ency limit of the spectra. The corresponding equivalent circuit is given in Fig. 4. This equivalent circuit is relatively simple but accounts well for the presence of two time constants in the impedance diagrams. The double layer capacitance was replaced by a constant phase element (CPE). This complex element was frequently used in order to take into account the frequency dispersion normally observed. The impedance of a CPE is given by :

$$Z_{CPE} = Z_0(j\omega)^{-n}$$

where Z_0 is the adjustable parameter used in the non-linear least squares fitting and the factor n, defined as a CPE power, is the adjustable parameter that always lies between 0.5 and 1. It can be obtained from the slope of [Z] on the Bode plot. When n = 1, the CPE describes an ideal capacitor. For 0.5 < n < 1, the CPE describes a distribution of dielectric relaxation times in frequency space, and when n = 0.5, the CPE represents a Warburg impedance with diffusional character.

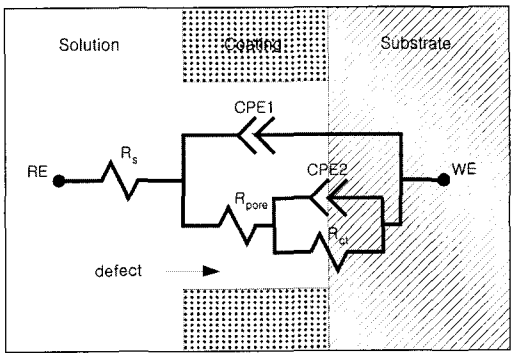

Fig. 4 Equivalent circuit for describing the impedance behavior of Type 304 SS coatings (R_S, electrolytic resistance; R_P, electrolytic resistance through the coating pores; R_{ct}, charge transfer resistance; CPE, constant phase element (CPE1, capacitance of the film; CPE2, double layer capacity) RE, WE, reference and working electrodes).

Usually if the value of n is 0.8 or more the element can be viewed as a capacitor.

Also, the value of n may be affected by the roughness and quality of the electrode, and by the placement and size[18, 19]. The values of the relevant parameters are summarized in Table 3.

From the impedance measurements carried out for each system, the values of the parameters R and C were considered in order to follow the modification of the properties of the coating with immersion time and the protection afforded by the different coatings. The coating capacitance is generally considered to provide information on the degree of water penetration through the coating and, in principle, its value is expected to increase with immersion[20]. Fig. 5 presents the evolution of C_{coat} against the immersion time. The capacitance values increased with immersion time. This behavior is in agreement with electrolyte uptake of the coatings. For C3a (40W/㎠, -0V) samples, capacitance had higher values than others. It is obvious that the penetration and diffusion of electrolyte through C3a coating was easier than others. The charge transfer resistance of the surface layer is shown in Fig. 6.

Usually, the values of R_{ct} decreased steadily

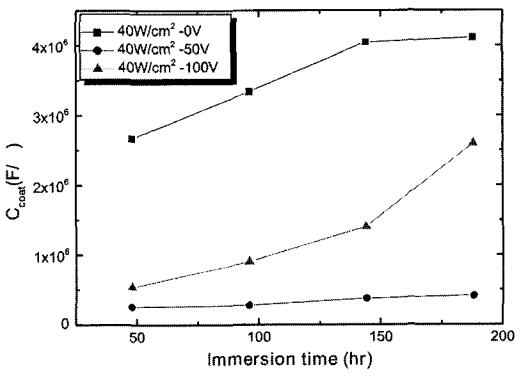

Fig. 5 Evolution of Ccoat with immersion time.

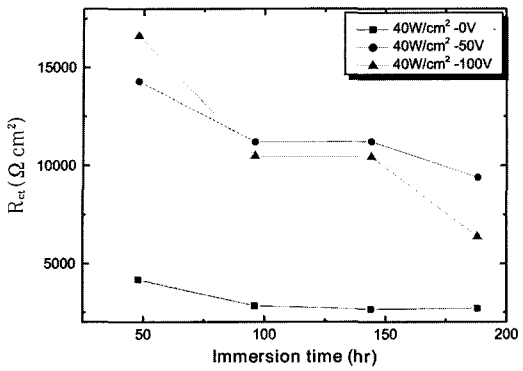

Fig. 6. Evolution of R_{ct} with immersion time.

with immersion time[21]. This phenomenon is in agreement with an increase in the number of pores which increases the area in contact with the electrolyte. C3c (40W/㎠, -100V) and C3b (40W/㎠, -50V) coatings had higher charge transfer resistance than C3a (40W/㎠, -0V) coating, which implies that these coatings showed higher corrosion resistance. Also, as is evident from rapid decrease of the R_{ct} value of C3c coating with exposure time, C3b coating showed better corrosion resistance as compared to C3c coating. This result was consistent with the previous test results.

Fig. 7 shows the experimental data for C3c (40W/㎠, -100V) coating represented in the form of Nyquist diagram and fitted curve. The fitted curve shown the solid line was in good agreement with the experimental data.

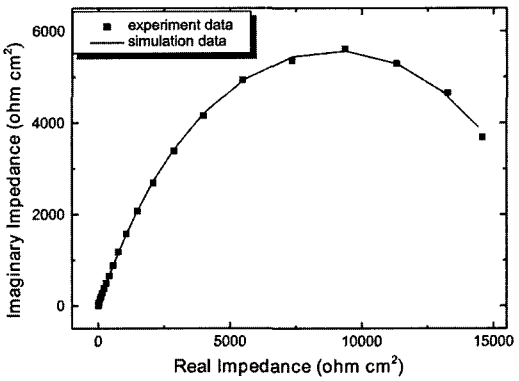

Fig. 7 Simulation for EIS data of the C3c (40 W/cm² -100 V) using the transfer function for the equivalent circuit of Fig. 4.

Table 3. Electrochemical parameters obtained by the equivalent circuit simulation.

Exposure time		R_s (Ω㎠)	CPE1		R_{coat} (Ω㎠)	CPE2		R_{ct} (Ω㎠)
			C_{coat} ($\times 10^{-5}$F/㎠)	n (0-1)		C_{pore} ($\times 10^{-5}$F/㎠)	n (0-1)	
C1	1 day	2.304	9.6572	0.845	680.3	16.124	0.757	6217
	3 day	2.072	10.433	0.870	462.6	43.915	0.716	4319
	8 day	4.337	15.067	0.845	376.6	146.58	0.640	2805
C2	1 day	5.697	4.1373	0.818	335.5	10.122	0.754	6927
	3 day	3.629	10.608	0.715	96.21	22.492	0.746	6653
	8 day	3.911	15.456	0.719	94.95	33.347	0.773	5102
C3a	1 day	5.078	26.687	0.809	522.0	15.983	0.820	4169
	3 day	2.607	32.212	0.781	504.3	22.703	0.844	3911
	8 day	3.688	41.132	0.741	344.3	77.137	0.879	2701
C3b	1 day	3.119	2.4364	0.903	335.9	6.9972	0.769	22738
	3 day	3.104	2.6831	0.899	401.5	19.766	0.751	12985
	8 day	2.886	4.1381	0.866	290.8	47.65	0.735	9396
C3c	1 day	4.765	5.2377	0.787	1423	6.0464	0.665	16384
	3 day	6.604	6.2446	0.749	1156	17.500	0.664	12711
	8 day	6.754	25.966	0.701	331.1	41.977	0.671	6381

3. 4 SEM and EDS

After the completion of immersion tests, the morphology and corrosion features of each coated system were inspected by SEM and the resulting micrographs are shown in Fig. 8. This figure showed many corrosion products resulting from

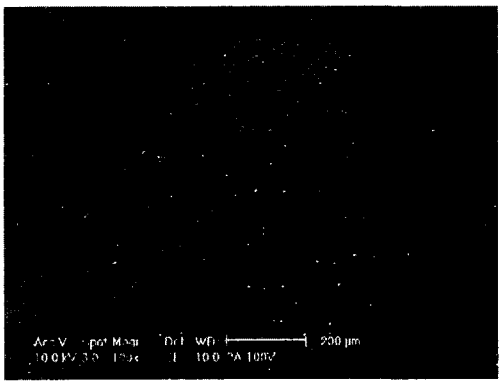

(a) C1 (11 W/cm^2 -100 V)

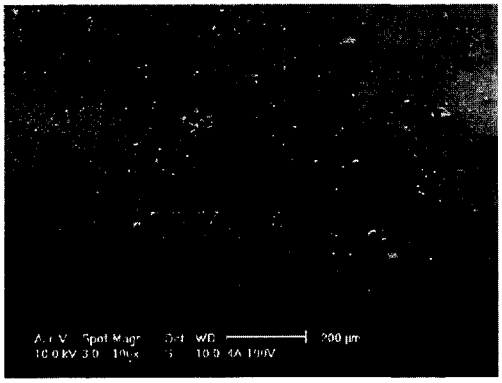

(b) C2 (25 W/cm^2 -100 V)

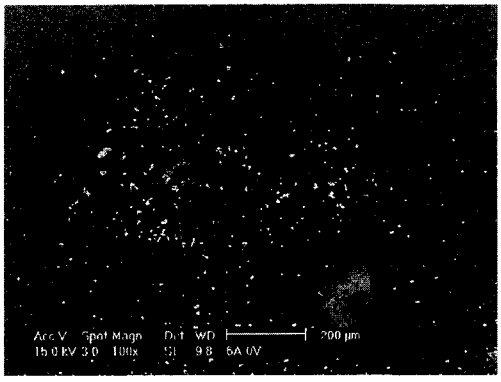

(c) C3a (40 W/cm^2 -0 V)

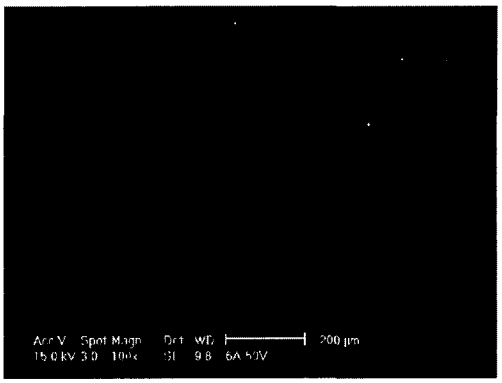

(d) C3b (40 W/cm^2 -50 V)

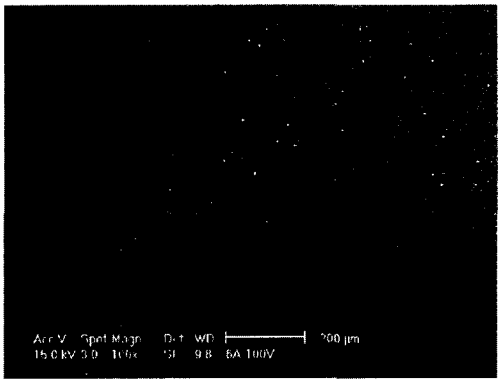

(e) C3c (40 W/cm^2 -100 V)

Fig. 8 Surface morphologies of specimens after the immersion test.

the dissolution of the substrate through the porosity of coating. The dark parts of C3c (40W/cm^2, -100V) interestingly showed the spots where the coating had flaked off. Qualitative EDS analysis indicated the presence of the expected elements in the corrosion products: i.e. Fe, O, Cr and Ni.

4. Conclusions

The investigation of Type 304 SS coating deposited using unbalanced magnetron sputtering (UBMS) shows the following results:

1) The sputtered Type 304 SS films exhibited a ferritic b.c.c. á-phase, though the bulk 304 SS is

an austenitic phase.

2) The corrosion behavior of Type 304 SS coatings was controlled by the power density and the bais voltage. All the coated samples presented a better corrosion resistance regarding the substrate.

3) At the applied frequency range, the equivalent circuit employed for the description of the EIS spectra for the coated steel provides the best fit of the experimental data. The capacitance values increased with immersion time and the C_{coat} of the C3a (40W/㎠, -0V) had higher values than others. But the charge transfer resistance values decreased with immersion time and the R_{ct} of C3b (40W/㎠, -50V) had the highest values.

4) An optimized deposition condition for corrosion protection was found as 40W/㎠ and -50V, which depends on good adhesion and low porosity of coating.

Acknowledgments

The authors are grateful for the support provided by the Korea Science and Engineering Foundation through the Center for Advanced Plasma Surface Technology at SungKyunKwan University.

References

1. M. L. Lau, E. J. Lavernia, Mater. Sci. Eng. A 272 (1999) 222.
2. B. Navinsek, P. Panjan, I. Milosev, Surf. Coat. Technol. 116-119 (1999) 476.
3. B. A. Shedden, F. N. Kaul, M. Samandi, B. Window, Surf. Coat. Technol. 97 (1997) 102.
4. K. He, H. Gong, K. Zeng, Z. Li, W. Gao, Mater. Let. 46 (2000) 53.
5. P. J. Kelly, R. D. Arnell, Surf. Coat. Technol. 98 (1998) 1370.
6. L. Cunha, M. Andritschky, Surf. Coat. Technol. 111 (1999) 158.
7. H. A. Jehn, Surf. Coat. Technol. 125 (2000) 212.
8. P. K. Vencovsky, R. Sanchez, J. R. T. Branco, M. Galvano, Surf. Coat. Technol. 108-109 (1998) 599.
9. G. Bertrand, H. Mahdjoub, C. Meunier, Surf. Coat. Technol. 126 (2000) 199.
10. C. Liu, A. Leyland, S. Lyon, A. Matthews, Surf. Coat. Technol. 76-77 (1995) 623.
11. J. Creus et al., Surf. Eng. 14 (1998) 432.
12. M. Tomlinson, S. B. Lyon, P. Hovsepian, W. D. Munz, Vacuum 53 (1999) 117.
13. M. Idiri et al., Surf. Coat. Technol. 122 (1999) 230.
14. W. Brandl, C. Gendig, Thin Solid Films 290-291 (1996) 343.
15. Denny A. Jones, Principles and Prevention of Corrosion, Prentice-Hall, London, 1996, p. 169-177
16. J. Y. Chen, G. P. Yu, J. H. Huang, Mater. Chem. Phys. 65 (2000) 310.
17. W. Tato, D. Landolt, J. Electrochem. Soc. 145 (1998) 4173.
18. E. M. A. Martini, I. L. Muller, Corros. Sci. 42 (2000) 443.
19. Barry C. Syrett, Electrochemical Impedance and Noise, NACE, NewYork, 1995, p. 43-45
20. C. Corfias, N. Pebere, C. Lacabanne, Corros. Sci. 41 (1999) 1539.
21. F. Mansfeld, M. W. Kendig, S. Tsal, Corrosion 38 (1982) 478.